

# PRIMARY FREQUENCY CONTROL PARTICIPATION PROVIDED BY DOUBLY FED INDUCTION WIND GENERATORS

Rogério G. de Almeida  
INESC PORTO  
Porto, Portugal  
ralmeida@inescporto.pt

J. A. Peças Lopes  
INESC PORTO - FEUP  
Porto, Portugal  
jpl@fe.up.pt

**Abstract** – This paper describes a control approach applied on doubly fed induction generator (DFIG) to provide a frequency regulation capability. The control scheme proposed consists in the integration into active power control loop of the rotor controller of an additional control loop responding proportionally to the system frequency deviation providing a primary frequency regulation capability. This strategy was exploited to allow wind power penetration in large isolated grids.

**Keywords** *Wind generation, frequency control, system dynamic behavior*

## 1 INTRODUCTION

Wind generation tends to play an important role in the total generation mix of the future power system due the need to decrease CO<sub>2</sub> emissions resulting from electricity production. This wind generation can appear in large concentrations of wind turbines (on-shore and off-shore), directly connected to the transmission grid, or as dispersed generation (DG) units spread through distribution grids.

Since wind power is supplied from a fluctuating primary energy source – the wind - the presence of such a large amount of generation in the system may have influence on the system dynamic response following generation imbalance and or grid disturbances. Most of these concerns are related with the management and control of primary and secondary reserves.

Such facts are receiving lately considerable attention from electric utilities in several countries leading to the definition of new Grid Code requirements for wind farms, namely regarding ride through default capabilities and fast active power frequency response.

Among the different wind energy conversion (WEC) systems used [1-2], double fed induction generators (DFIG) are capable of providing the required capabilities without the need of large costs on the power electronics hardware, provided that adequate control strategies are added.

The control flexibility provided by the DFIG electronic converter makes it possible to define various control strategies for participation in primary frequency control. In previous works, described in [3-4], the capability of the DFIG in responding to changes in network frequency is described, assuming a previous de-load regarding the maximum torque extraction curve. In these works a supplementary control loop, that uses as addi-

tional input variables the derivative of the system frequency or the derivative of kinetic energy at any speed, was adopted providing also an inertia response similar to that of a synchronous generator. The feasibility of these control strategies was demonstrated through numerical simulations performed in simple systems.

In this work these DFIG control concepts are exploited and used to provide additional support to primary frequency control allowing the increase of the level of wind power penetration in large isolated systems. The control approach adopted consists in the use of an additional frequency control loop that is integrated into the rotor-side active power controller of a DFIG.

In this control scheme a small de-load regarding the maximum power extraction curve of the wind generator is implemented to allow its participation in frequency control during an eventual decrease of system frequency. To complete the control approach, a pitch control strategy is also included and dominates the power control for high wind speeds.

Different types of system disturbances like short-circuits and load increase are applied in a medium size isolated test system, in order to evaluate the effectiveness and the advantages of the use of this frequency control scheme obtained from the DFIG. An evaluation of the use of this DFIG control approach to increase wind power penetration in this medium size test grid is discussed.

## 2 STRUCTURE OF THE WEC SYSTEM

### 2.1 Doubly Fed Induction Generator Control

Figure 1 depicts the general scheme of the DFIG, converters and controllers exploited in this work. A full description of the DFIG mathematical model used in this research is given in [5].

A  $d-q$  voltage regulator is adopted for the control of the rotor-side converter, modeled as voltage source. To achieve active / reactive power control capabilities the rotor-side converter operates in a stator-flux  $d-q$  reference frame, controlling both active and reactive power outputs through  $v_{qr}$  and  $v_{dr}$  components, obtained from two separate sets of PI controllers. More details of this scheme are described in [6]. The PI controllers involve a cascade structure, where the outside PI blocks are used to regulate the reference rotor currents ( $i_{qref}$  and  $i_{dref}$ ) and



The calculation of the optimal power coefficient,  $C_{p_{opt}}$ , can be obtained from the following function as suggested in [2]:

$$C_{p_{opt}}(\lambda_{opt}, \theta) = 0.22 \left( \frac{116}{\lambda_t} - 0.4\theta - 5 \right) e^{-\frac{12.5}{\lambda_t}} \quad (7)$$

$$\frac{1}{\lambda_t} = \frac{1}{\lambda_{opt} + 0.08\theta} - \frac{0.035}{\theta^3 + 1} \quad (8)$$

The optimal tip speed ratio is defined as

$$\lambda_{opt} = \frac{\omega_{t_{opt}} R}{U_w} \quad (9)$$

Where  $R$  (m) is the blade radius and  $\omega_{t_{opt}}$  is the optimal wind turbine rotor speed (rad\_mec/s) for a given wind speed.

From (6) and (9) an optimum (maximum) power value -  $P_{opt}$  - can be obtained as a function of the shaft speed, referred to the generator side of the gearbox, as follows:

$$P_{opt} = k_{opt} \omega_r^3 \quad (10)$$

Where,  $k_{opt} = \left(\frac{1}{2}\right) \rho (C_{p_{opt}} / \lambda_{opt}^3) \pi R^5$ ,  $\omega_r = (p/2)G\omega_t$ , being  $p$  number of poles and  $G$  the transmission ratio of gearbox.

From (10) the wind turbine pre-defined optimal extraction power curve can be established for a given  $k_{opt}$  associated to a fixed blade angle which should be defined for an averaged short term wind speed forecast. Such approach was adopted here because it was assumed that the site where wind turbines were installed was characterized by some strong winds, which requires an adjustment on the blade pitch angle to extract maximum power in those conditions.

In this research wind farms constituted by 12 and 15 wind turbines were considered. Individual data of these generators is described in the Annex. For both wind parks  $k_{opt}$  is defined for a fixed blade angle equal to 16 degrees, assuming that a short term wind speed forecast was available. In Figure 3 the pre-defined maximum extraction power curves adopted for both wind parks, as used in the control procedure described next, are shown.

### 2.3 Primary frequency control

The primary frequency control integrated into the rotor-side active power control loop is similar to the one usually used in synchronous generators. In this case, the droop loop (characterized by a regulation  $R$ , expressed in p.u. in the system base) is used to produce a change in the active power injected by the DFIG when a system frequency variation occurs. The active power increment is therefore proportional to the system frequency variation and is defined as:

$$P_{injected} = P_{ref} - \frac{1}{R} (\underbrace{\omega_{sys} - \omega_{sys\_ref}}_{\Delta P \text{ increment}}) \quad (11)$$

This generated active power requires a new operating point of the DFIG, characterized by a new rotational speed and mechanical power to be identified in the power curve of a given wind speed (Figure 3).

The input reference active power of the DFIG active power loop is initially obtained from a 5% de-loaded maximum power extraction curve, defined in Figure 3, considering the rotational speed referred to the generator side. For large de-loads combined operation of the pitch control and of the electronic converter control should be used, as described in [4]. Such approach allows an active power injection from the DFIG when the system frequency decreases. Figure 4 depicts the full control approach adopted for the rotor-side.

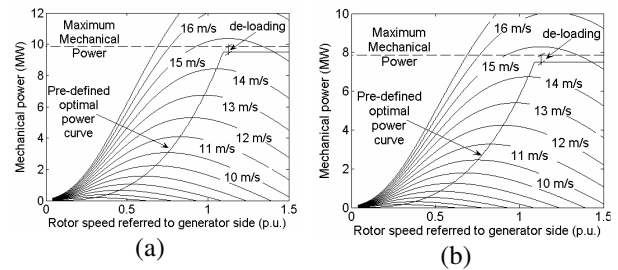


**Figure 3:** Pre-defined power curves for: (a) wind park with 15 turbines; (b) wind park with 12 turbine.

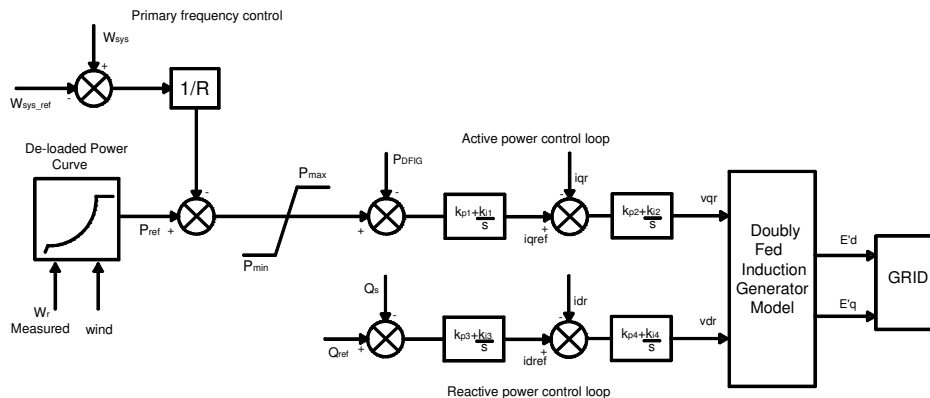


**Figure 4:** General schematic of the rotor-side PI controllers and primary frequency control.

## 2.4 Pitch control

For wind speeds below maximum rated speed (according to the operational optimal power curve) the input reference active power to the active power loop in DFIG follows the eqn. (11) as discussed in a previous section. However, for wind speeds larger than maximum rated speed, the blade pitch regulation dominates the control and limits the energy captured from the turbine. In this case, the pitch control (shown in detail in [1]) will control the rotor speed referred to the generator side and will operate until the wind cut-off speed limit is reached. The input speed reference for pitch control is defined according to [6]:

$$\text{If } P_{mec} \geq P_{max} \text{ then } \omega_{ref} = \frac{P_{max}}{T_{mec}} \quad (12)$$

## 3 SIMULATION RESULTS

Figure 5 shows the power system used to evaluate the performance of the general control approach described previously. It includes one large steam unit, two Diesels and one hydro generator and four wind farms. These wind farms are constituted by 12 or 15 DFIG, as described in Figure 5. Equivalent DFIG were used to represent each wind park. The procedure used to obtain the electromechanical equivalent of the wind parks are full described in [10]. The parameters of each wind generator are presented in Annex.

Two distinct operation scenarios were considered: 1) wind generators were assumed to be DFIG without frequency regulation control; 2) the described control approach was supposed to be included in all the DFIG. The overall capacity of the wind parks represents approximately about 27 % of the total installed generation.

To perform the dynamic behavior analysis of this system a full mathematical description of the electrical and mechanical behavior of the synchronous units connected to bus 0, 2, and 9 was also used. Synchronous generators were represented through a fifth-order transient model together with an automatic voltage regulator (IEEE type 1) and a speed governor with proportional and integral frequency control. A single first order model represents the steam turbine and the equivalent of the two Diesel motors, as described in [8]. A linear model (without transient droop), described in [9], was used to represent the hydraulic unit behavior. The impedance matrix model developed in [10] is used to describe, in a compact form, the coupling between the transmission network and the machines stator equations.

Conventional synchronous units use a 5% droop value (in each machine base). The network data and synchronous units data can be obtained from the authors upon request.

Two types of disturbances were simulated to evaluate the contribution from DFIG to increase system robustness.

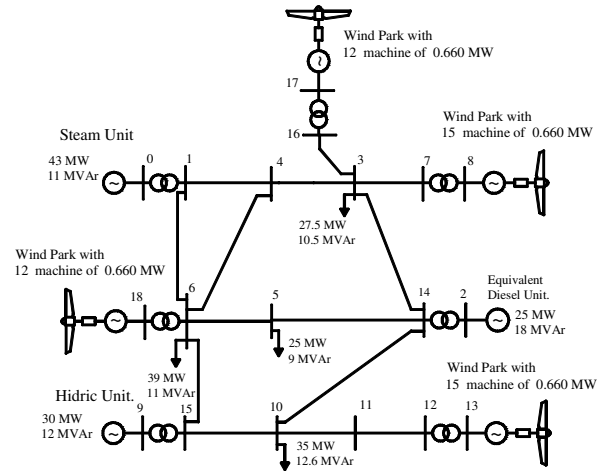


Figure 5: Single line diagram of the test power system

These disturbances were as follows: a) load step increase at bus-bar 5; and b) symmetrical impedant three-phase short circuit at bus-bar 10. Due to space limitations, only the behavior of the wind parks connected at bus bar 13 (with 15 wind turbines) and bus bar 17 (with 12 wind turbines) will be presented. Wind speed is assumed to be constant (for cases a and b) and equal to 14 m/s and 13 m/s for wind parks of busses 13 and 17, respectively.

### 3.1 Load increase

A load increase was simulated through a sudden step increase of 50% of the load in bus bar 5, at  $t = 1$  second. This corresponds to a total increase in the system load of about 10%.

#### Initial scenario

An initial system scenario was considered assuming that all synchronous units were in operation and that wind power penetration was about 21%.

Results: Figure 6 illustrates the system frequency behavior with and without wind farms participating in primary frequency regulation.

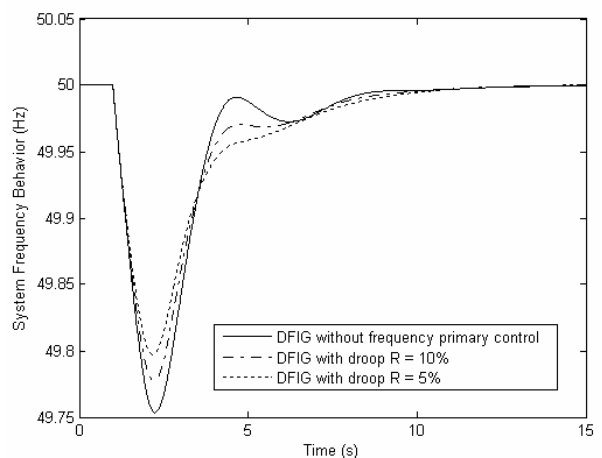


Figure 6: System frequency behavior for DFIG with and without participation in primary frequency control.

Different droop ( $R$ ) values were used (5 % and 10%, in the machine base). The frequency integral control of the synchronous units brings frequency back to its nominal value.

When frequency drops because of the load increase, wind farms with primary frequency control are sharing with the conventional units the frequency regulation task, improving in this way the overall system response. A droop of 10% used by the DFIG has already provided some support to the system during the first moments that follow the disturbance. A 5% droop leads to a larger injection of active power increasing system robustness of operation.

In this case, the DFIG primary frequency control imposes an active power increment that is added to the reference input, obtained from de-loaded maximum extraction power curve (see Figure 3). As a result, the rotor speed falls, transferring kinetic energy into the grid and compensating the increase of active power injected by the DFIG. Since the power increment signal (defined in equation 11) becomes zero, following the integral frequency control actuation of the synchronous units, the wind turbine is driven to operate again nearer the reference optimum mechanical power. If the integral frequency control of the synchronous units was not in operation the DFIG would increase its active output power, sharing the load increase with the synchronous units.

If an additional secondary frequency control signal, defined by a wind park control, responding to an AGC request, was added to the first adder of Figure 4 it would be possible to have also wind generators participating in frequency control.

Figures 7 and 8 show the behavior of the injected active powers and rotor speeds of wind farms connected to bus bars 13 and 17, respectively.

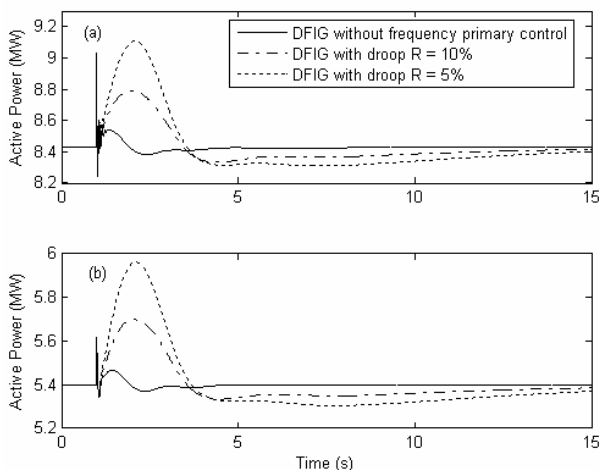


**Figure 7:** Active power injected by wind farm connected: (a) at bus-bar 13; (b) at bus-bar 17.

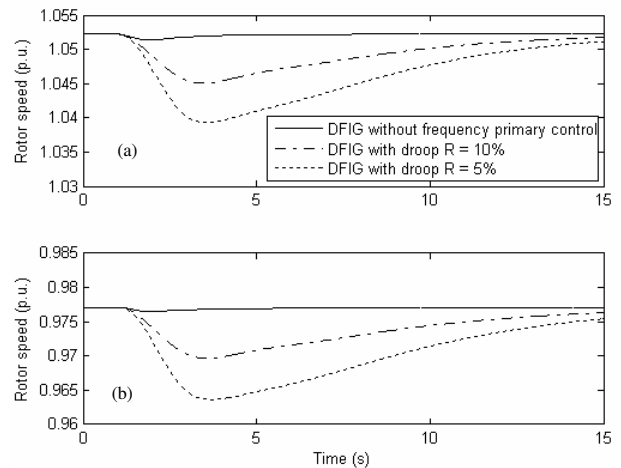


**Figure 8:** Rotor speed in wind farm connected: (a) at bus-bar 13; (b) at bus-bar 17.

#### Increasing wind power generation scenario

Conventional synchronous units supply the major portion of the active power consumed by grid and are responsible for reestablish the overall system frequency. So a reduction of the number of synchronous units in operation significantly affects the overall frequency regulation capability and can contribute to reduce system robustness regarding disturbances.

In this simulation case it was assumed that the Diesel power station is out of service, being replaced by an increase from wind power generation, which requires an increase in the number of wind turbines installed.

Two cases were analyzed: 1) the system with the Diesel units and operating without increase of new wind generation, corresponding to a wind penetration of 21,7%; and 2) new wind generators are installed in order to compensate the lack of the Diesel units, increasing wind power penetration to 38,2%.

In both cases, DFIG with or without frequency primary control are considered. The wind farm characteristics for both simulation cases are resumed in Table 1.

SIMULATION CONDITIONS					
First case			Second case		
Bus bar	Rating (MW)	Wind speed (m/s)	Bus bar	Generation (MW)	Wind speed (m/s)
8	8.43	14	8	14.04	14
13	8.43	14	13	14.04	14
17	5.4	13	17	9	13
18	6.74	14	18	11.24	14
Total	29			48.32	
INCREASING OF DFIG (Second case)					
Bus bar		Wind generators added			
8 and 13		10			
17 and 18		8			

**Table 1:** Data concerning wind farms for the considered simulation cases.

**Results:** At  $t = 1$  second, a load increase, as described in the previous section, is applied. The droop value used by the DFIG in these simulations is 5% (in the machine base). The system frequency behavior is shown in Figure 9. It can be observed that when wind farms do participate in primary frequency control an expressive enhancement of system response is clearly obtained. The replacement of Diesel generation by wind generation does not reduce system robustness of operation, provided that the required wind power is available.

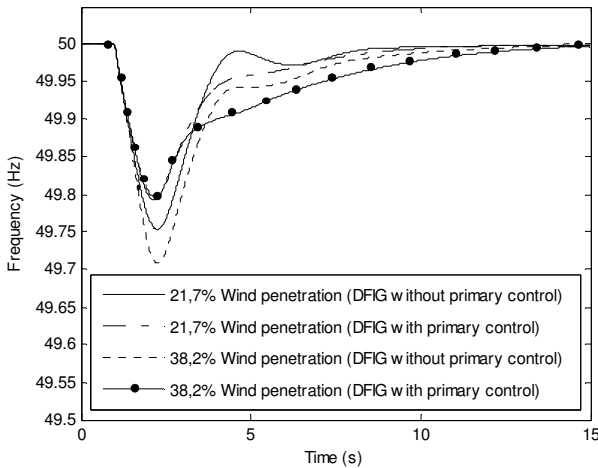


**Figure 9:** System frequency behavior concerning Diesel unit turned off and wind farms with or without increasing of connected DFIG.

### 3.2 Symmetrical Impedant Three Phase Short Circuit.

In order to evaluate the impact of the DFIG primary frequency control during a short circuit it was assumed that the wind generators and their electronic converters were able to withstand this system default (ride through default capability). A typical short-circuit clearing time equal to 100 ms was assumed.

**Results:** At  $t = 1$  second a symmetrical impedant short circuit is applied at bus-bars 10 using the initial scenario defined in section 3.1. Figures 10-12 depict the system frequency behavior, the active power, and rotor speed following the short circuit, respectively.

In this simulation case, it is observed that the primary frequency control responds quickly and helps to improve slightly the system frequency response. During the short circuit the overall system response is more or less the same with and without DFIG participating in primary frequency control. A better damping performance is obtained for the case where DFIG adopt the smallest droop, as shown in Figure 10, because after fault elimination the DFIG participating in primary frequency control leads to an increase in active power injection. In this case a larger power increment is added to the reference active power input when the system frequency decreases as shown in Figure 11. This fact makes it possible for the conventional synchronous units to respond by injecting less active power into the grid, thereby improving the system frequency smoothly. As discussed in the load increase case, when the power

increment increases the rotor active power also increases and, consequently, the rotor speed tends to fall a little more after fault elimination balancing the total active power ( $P_{stator} + P_{rotor}$ ) injected by DFIG as illustrated in Figure 12.

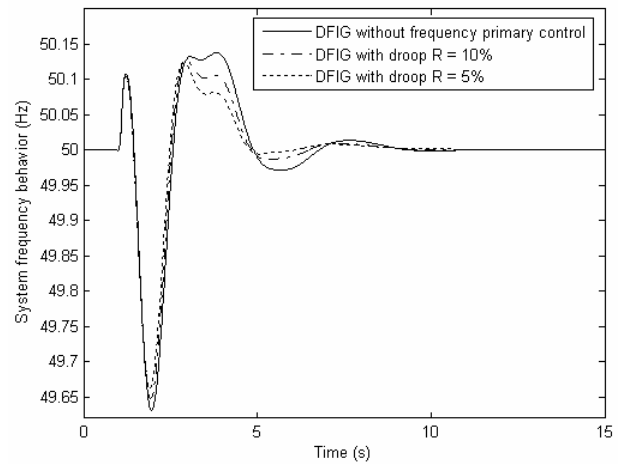


**Figure 10:** Frequency behavior during a symmetrical impedante fault.

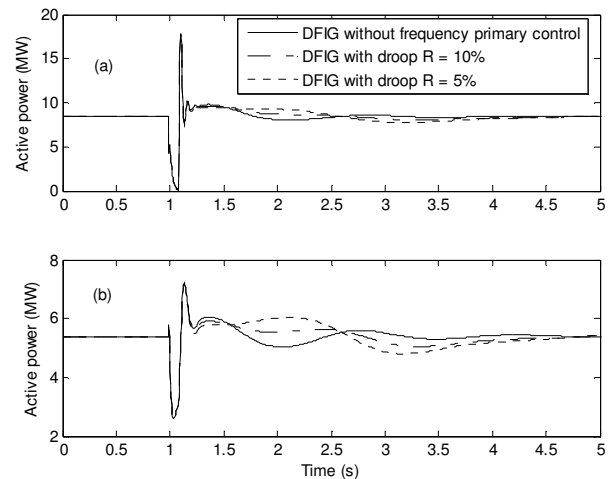


**Figure 11:** Active power injected during symmetrical impedante fault by wind farms connected: (a) at bus-bar 13; (b) at bus-bar 17.

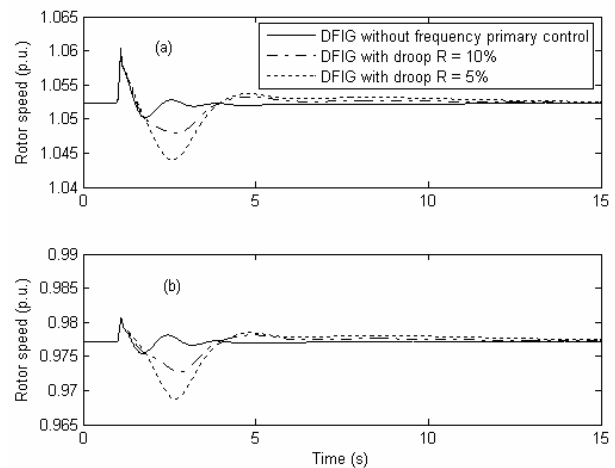


**Figure 12:** Rotor speed during symmetrical impedante fault in wind farm connected: (a) at bus-bar 13; (b) at bus-bar 17.

## 4 CONCLUSIONS

In this work the impact in an isolated system of the use of a primary frequency control strategy, integrated into a DFIG active power control loop and exploiting the system frequency deviation as input signal, was addressed. A detailed description of the used control approach was provided and discussed.

It was shown that the fact of having wind generators participating in the frequency control may contribute to increase system robustness, reducing frequency changes following disturbances. Such a control approach allows increasing wind power penetration in the system (either as distributed generation or in large wind parks).

Having in mind the increase in the penetration of wind generation in power system, namely using DFIG technology, such a control approach can play a key role in providing the necessary system robustness.

## ACKNOWLEDGMENT

The authors would like to acknowledge Fundação para Ciência e Tecnologia of Portugal (FCT) by its support under the framework of the DIPTUNE POCTI741614/ESE/2001 project.

## ANNEX

### A. *Parameters:*

Base values for the per-unit system conversion.

Base Power: 100 MVA

Base Voltages: 0.69 kV for low-voltage bus-bar, 33 kV for medium-voltage bus-bar and 63 kV for high voltage bus-bar.

### B. *Doubly Fed Induction Generator:*

$P_n$ (kW) = 660,  $V_n$ (kV) = 0.69,  $R_s$ (p.u.) = 0.067,  $X_s$ (p.u.) = 0.03,  $R_r$ (p.u.) = 0.0058,  $X_r$ (p.u.) = 0.0506,  $X_m$ (p.u.) = 2.3161,  $\omega_s$ (r.p.m) = 1500, No of poles = 4, rated slip generator = 2% , DC Voltage = 326.60 V, Capacitor = 284  $\mu$ F , Rotor transformer reactance = 9.5%,

### C. *Wind Turbine:*

No. of blades = 3, Rotor diameter = 22 m, cut-in seed = 4 m/s, cut-off speed = 25 m/s, Atm. density = 1.225  $\text{Kg.m}^{-3}$ , Inertia time constant = 4, Gear box ratio 1: 60

### D. *Clark's Transformation (a-b-c) $\rightarrow$ ( $\alpha$ - $\beta$ -0):*

$$\begin{bmatrix} V_0 \\ V_\alpha \\ V_\beta \end{bmatrix} = \sqrt{\frac{2}{3}} \begin{bmatrix} 1/2 & 1/2 & 1/2 \\ 1 & -1/2 & -1/2 \\ 0 & \sqrt{3}/2 & -\sqrt{3}/2 \end{bmatrix} \begin{bmatrix} V_a \\ V_b \\ V_c \end{bmatrix}$$

And,

$$\begin{bmatrix} V_a \\ V_b \\ V_c \end{bmatrix} = \sqrt{\frac{2}{3}} \begin{bmatrix} 1/2 & 1 & 0 \\ 1/2 & -1/2 & \sqrt{3}/2 \\ 1/2 & -1/2 & -\sqrt{3}/2 \end{bmatrix} \begin{bmatrix} V_0 \\ V_\alpha \\ V_\beta \end{bmatrix}$$

Similar expressions can be defined for the currents.

## REFERENCES

- [1] V. Akhmatov, "Analysis of Dynamic Behavior of Electric Power System with Large Amount of Wind Power", PhD Thesis, April 2003.
- [2] J. G. Slootweg, S. W. H. de Haan, H. Polinder and W. L. Kling, "Modelling Wind Turbine in Power System Dynamics Simulations", 2001 IEEE Power Engineering Society Summer Meeting, Vancouver, Canada, July 15-19, 2001.
- [3] J. Ekanayake and N. Jenkins, "Comparison of the Response of Doubly Fed and Fixed-Speed Induction Generator Wind Turbines to Changes in Network Frequency", IEEE Transactions on Energy conversion, vol. 19, No. 4, pp. 800-802, December 2004.
- [4] J. Ekanayake, L. Holdsworth and N. Jenkins, "Control of DFIG Wind Turbines", Power Engineering Journal, vol. 17, No 1, pp. 28-32, February 2003.
- [5] R. G de Almeida, J. A. Peças Lopes and J. A. L. Barreiros, "Improving Power System Dynamic Behavior Through Doubly Fed Induction Machines controlled by Static Converter Using Fuzzy Control", IEEE Transactions on Power System, vol. 19, No. 4, November 2004.
- [6] R. Pena, J. C. Clare and G. M. Asher, "Doubly Fed Induction Generator Using Back-to-Back PWM Converters and its Applications to Variable-Speed Wind-Energy Generation", IEE Proc-Electric Power Application, vol. 143, No 3, May 1996.
- [7] H. Akagi *et al.*, "Instantaneous reactive power compensators comprising switching devices without energy storage components", IEEE Trans. Ind. Application, vol. IA-20, pp. 625-630, May/June 1984.
- [8] P. Kundur, "Power System Stability and Control", New York: McGraw-Hill, 1994.
- [9] D. G. Ramey and J. W. Skooglund, "Detailed Hydrogovernor Representation for System Stability Studies", IEEE Press - Stability of Large Electric Power System, 1974.
- [10] G.S. Stavrakakis and G. N. Kariniotakis, "A General Simulation Algorithm for the Accurate Assessment of Isolated Diesel-Wind Turbine Systems Interaction - Part I: A General Multimachine Power System Model", IEEE Trans. Energy Conversion, vol. 10, pp. 577-583, September 1995.